UDC 622.24.053.6
DOI: 10.15587/2312-8372.2019.156746

Rachkevych R.,
Ivasiv V.,
Bui V.,
Yurych L.,
Rachkevych I.

LABORATORY RESEARCH OF THE STRESS-STRAIN STATE OF THE DRILL STRING IN THE LOCAL BEND OF THE WELL

Об'єктом дослідження даної роботи є експлуатація бурильної колони в локальному перегині свердловини. Одним із найбільш проблемних аспектів у даному випадку вважається встановлення її напружено-деформованого стану. Це надзвичайно важлива інформація, яка, зокрема, використовується для прийняття рішень щодо тривалості та можливості експлуатації бурильної колони в заданих геолого-технічних умовах.

Опираючись на критичний огляд літератури, для вирішення вказаної проблеми обрано фізичне моделювання об'єкту дослідження. Зокрема, було спроектовано, виготовлено та апробовано спеціальний лабораторний стенд, який забезпечує:

– навантаження моделі бурильної колони осьовою силою розтягу й крутним моментом;

– моделювання криволінійних осей свердловин із можливими локальними перегинами, опираючись на результати промислової інклінометрії та профілеметрії;

– вимірювання напружень і деформацій моделі колони та їх інтерпретація до величин натурного об'єкту.

В якості моделі бурильної колони використано мідну трубку із обважнювачем для забезпечення критеріальної подібності із натурним об'єктом. Для вимірювання нормальних напружень на моделі бурильної колони використано метод тензометрування. При цьому, аналогові значення напруг на тензодавачах оцифровуються та передаються на персональний комп'ютер для подальшого оброблення й інтерпретації.

За допомогою запропонованого лабораторного стенду було проведено експериментальні дослідження напружено-деформованого стану моделі бурильної колони діаметром 127 мм в локальному перегині свердловини No. 10 Одеського родовища (Україна). Встановлено, що нормальні напруження від згину, які при цьому виникають, можуть більше ніж втричі перевищувати аналогічні величини, отримані без врахування наявності вказаного викривлення осі свердловини.

Завдяки запропонованому експериментальному методу забезпечується можливість дослідження деформацій і напружень, які виникають у бурильних колонах підчас їх роботи у свердловинах із локальними перегинами осей. При цьому немає необхідності застосовувати складні аналітичні перетворення та алгоритми. Крім того, модель має таку саму фізичну природу, як і об'єкт дослідження. Це є надзвичайно вагомим аргументом, особливо при дослідженні складних випадків взаємодії бурильної колони зі стінками свердловини.

Ключові слова: *напружено-деформований стан, бурильна колона, локальний перегин, лабораторне дослідження.*

1. Introduction

Oil and gas production is carried out by the construction of wells. In general, this is a deep, narrow hole of circular cross section in the soil, created with the help of special equipment without access to it by a person. The beginning of a well on the earth's surface is called the mouth, the bottom – the bottom. According to the position of the axis of the barrel and the well configuration are divided into vertical, horizontal and directional. The latter and the penultimate have curvilinear axes, often with sharp or local kinks, at which there is a rapid change in both zenith and azimuthal angles.

Of course, the main part of the above-mentioned equipment for the construction of wells is the drill string. From the point of view of mechanics, it is a lengthy object, the transverse dimensions of which are much smaller than the longitudinal ones. In addition, the drill string during operation is subjected to a wide range of loads. Among these are bending and torques, axial tensile and compressive forces, the effect of its own weight and the like. In addition, the deformation of the drill string is limited to the borehole walls. Such conditions lead to significant stresses in the cross section of the drill pipe. Often their value reaches the limit values, which can lead to emergency situations.

Therefore, one of the ways to overcome this problem is stopping the operation of the drill string before the onset of the limit state. This is possible under the condition of predicting its durability based on data on the stress-strain state. Consequently, the studies conducted in this paper do not raise doubts about their relevance.

2. The object of research and its technological audit

Summarizing the above, *the object of research* will be considered the operation of the drill string in the local well kink. One of the most problematic aspects in this case is the establishment of its stress-strain state.

In general, the interaction of drill pipe strings with the walls of a well under the action of applied external and

ISSN 2226-3780

internal loads is an extremely complex phenomenon. Its mathematical modeling requires time-consuming analytical transformations and is associated with significant methodological difficulties. This fully applies to the analysis of the stress-strain state of drill strings. In this case, for example, it is necessary to solve systems of differential equations of elastic equilibrium in the spatial formulation, without taking into account the hypothesis of small displacements.

At present, the use of the finite element method can be considered an alternative direction for solving this problem. It is a powerful tool for solving many problems of solid mechanics. However, the implementation of this approach requires the use of significant computing power and special software. In addition, when calculating drill columns of considerable length, taking into account most external factors and using a detailed grid of finite elements, it is possible and not to get the final result.

At the same time, the means and methods of physical modeling are free from these disadvantages. After all, they are based on the creation of a material model that has the same physical nature as the actual phenomenon.

3. The aim and objectives of research

The aim of research is design, manufacture and testing of a special laboratory test bench for studying the stress-strain state of a drill string model in a local well-bending.

For this it is necessary to solve the following objectives:

1. To provide criterion similarity between the drill string model and its full-scale object.

2. To develop a stand chassis design for modeling spatial distortions of the well axis in a sufficient range for practical needs in accordance with the results of industrial inclinometry and profilemetry.

3. To provide the load model of the drill string with the main external and internal factors: axial force, torque, borehole wall reactions, dead weight.

4. To conduct laboratory studies of the stress-strain state of a 127-mm drill string with its operation in the local bend of well No. 10 of the Odesa deposit (Ukraine) in order to quantitatively establish the effect of the latter on the stress-strain state of the string.

4. Research of existing solutions of the problem

Most often, the classical theory of bending [1] and the positions of the mechanics of flexible rods [2] are used for mathematical modeling of a drill string. The problem is solved in both flat and spatial formulation [3, 4]. But in the publication [5], special software based on the finite element method is used to analyze the stress-strain state of the drill string. However, it should be remembered that with an increase in compliance of the mathematical model with a real object, the equations for its description become significantly more complicated. This, in many cases, can be a counter-argument for choosing this particular approach.

On the other hand, physical modeling of the drill string is in many cases more appropriate. Let's consider the scientific potential in this direction.

The authors of [6] to analyze the shape of the elastic equilibrium of the drill string model in a straight wellbore conducted a corresponding laboratory experiment. Its essence was as follows. A flexible rod that simulates a drill string was placed in a transparent cylindrical cavity with a straight axis and loaded with axial force and torque. In the works [7, 8] the results of such studies are presented. For the analytical description of the elastic line of such rods, a sinusoidal curve and a spiral helix with constant or variable pitch are chosen. Both static and dynamic problem statements are considered. Let's note, however, that the results of such experiments can't be used to study the deformation of drill strings in curvilinear sections of wells.

However, the authors of [9] designed and manufactured a laboratory bench, which, among other things, allows to investigate the stress-strain state of a drill string in a well with an intensity change of the zenith angle from 1 to 6 degrees/100 m. Obviously, this value is not enough for practical needs, because the intensity of the curvature of real wells can reach from 1 to 6 degrees/10 m.

However, this fact was taken into account in [10]. The author presents a test bench for studying the stress-strain state of drill pipes with a diameter of 2 7/8 inches in a local well-bending (Fig. 1).

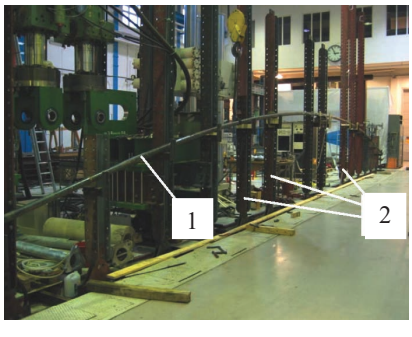

Fig. 1. General view of the experimental stand:
1 – drill string; 2 – tripods of the experimental stand

As can be seen from Fig. 1, using tripods, it is possible to realize a wide range of borehole curvature. Obviously, it is possible to conduct research in a flat and spatial formulation.

However, as can be seen from the design, problems may arise in the simulation of wells with axes with minor zenith angles. In addition, the design of the stand does not provide for imitation of the cross section of the wellbore. This means that it is impossible to take into account its effect on the stress-strain state of the drill string. In addition, there may be significant difficulties in the study of drill pipe strings of large sizes.

This work is devoted to overcoming the above disadvantages.

5. Methods of research

In [11], similarity criteria and the design of an experimental test bench are developed for the laboratory study of the stress-strain state of drill strings. Its general view along with a photo of the loading and support units is shown in Fig. 2, 3.

The experiment began with the fact that the simulators of the borehole wall 2 (Fig. 2) are set relative to the chassis in accordance with the inclinometric parameters of the considered well. For the enumeration of the length

measures between the natural well and its model, the dependence is used [11]:

$$\frac{L_M}{\mu_M} = \frac{L_F}{\mu_F},$$

where L – the length of the section of the drill string; μ – the length of one dimensionless unit of weight. The parameters that relate to the model are designated by the index «M», the full-scale object – «F».

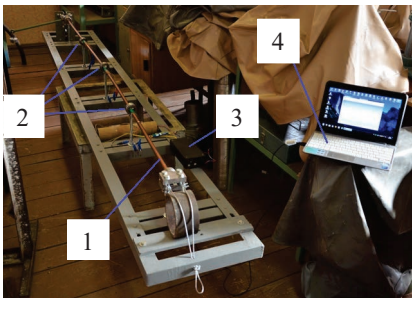

Fig. 2. General view of the experimental stand:
1 – model of a drill string in the form of a copper pipe with a filler;
2 – borehole wall simulators; 3 – analog-to-digital converter; 4 – personal computer

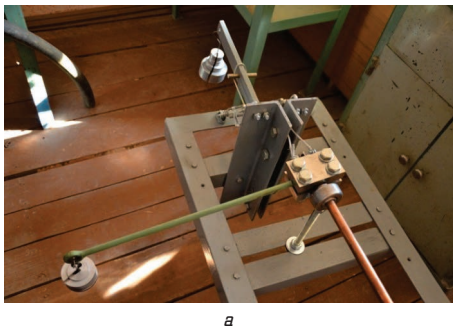

a

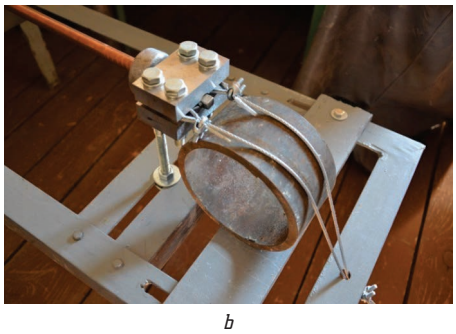

b

Fig. 3. Separate nodes of the experimental stand:
a – load unit; *b* – supporting unit

The determination of the axial force F and torque M, which load the drill string model, is carried out according to the formulas [11]:

$$\frac{F_M \mu_M^2}{E_M I_M} = \frac{F_F \mu_F^2}{E_F I_F}, \quad \frac{M_M \mu_M}{E_M I_M} = \frac{M_F \mu_F}{E_F I_F},$$

where E, I – the modulus of elasticity of the first kind of material and the moment of inertia of the cross-section of the drill string and its model.

Further, the copper pipe 1 is mounted in such a way that it passed through the holes of the simulators of the borehole wall 2 (Fig. 2). To study its stress state, strain gauging is used. Therefore, on the model of the drill string, in each place of contact with simulators of the borehole wall (except the extreme ones), strain gauges (GOST 21616-91) 15*a*, 15*b*, 15*c* and 15*d* are pasted as shown in Fig. 4.

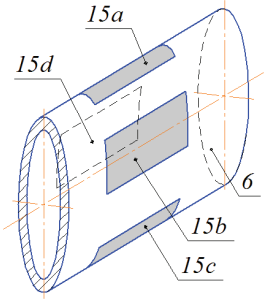

Fig. 4. Location of strain gauges on the surface of the drill string model: 15*a* – the first strain gauge; 15*b* – the second strain gauge; 15*c* – the third strain gauge; 15*d* – the fourth strain gauge

The next step, alternately carried out voltage measurements on all 12 strain gauges (four at each simulator of the borehole wall).

Further, the drill string model is returned to an angle of 90 degrees and fixed. As a result, strain gauges with an «*a*» index turns out to be in a position that before that was occupied by strain gauges with a «*d*» index. In turn, strain gauges «*b*» are in the position that before that occupied strain gauges «*a*» and again carrying out voltage measurement on all strain gauges.

A total of four turns are carried out at 90 degrees. This technique allows to measure at each point under control four times and avoid the effect of stress relaxation on the surface of the copper pipe.

The next step is calibration the strain gauges in order to obtain equality for converting the voltage into the corresponding voltage values.

Since the measuring strain gauges past on the cylindrical surface of the drill string model, it is decided to carry out the calibration in two stages. At the first stage, the calibration strain gauges are pasted directly onto the surface of the copper pipe. To carry out studies on the second stage, another fragment of the drill string model is compressed under a press so that a flat surface is formed on which the calibration strain gauges are also pasted.

Conducting such experimental studies will allow, in addition to obtaining a calibration characteristic, to establish the absence or presence of influence on the readings of strain gauges of the shape of the surface on which it is pasted.

So, both for the first and for the second stage, the studies are carried out using the same method, the essence of which is given below. Calibration strain gauge 2 is attached to the surface of a fragment of the drill string model 1 (Fig. 5). The fragment itself is fixed in a pincers 3 of a testing machine (Fig. 5). To prevent deformation of the experimental sample, a steel rod 4 is used (Fig. 5).

Each experimental sample is subjected to tension according to a predetermined set of load levels. In addition, for each value of the tensile force F_c, the stress is recorded on the calibration strain gauge U_c. Consequently, the function is obtained in discrete form:

$$U_c = f(F_c). \quad (1)$$

ISSN 2226-3780

For further use, equality (1) is transformed to the form:

$$U_c = f(\sigma_c), \quad (2)$$

where σ_c – the normal stress in the cross section of a fragment of the tubular model, equal to:

$$\sigma_c = \frac{F_c}{A},$$

where A – the cross-sectional area.

In the general case, the dependence (2) can be represented as a polynomial:

$$U_c = A_1\sigma_c + A_2\sigma_c^2 + ... + A_n\sigma_c^n, \quad (3)$$

where A_1, A_2,..., A_n – the coefficients of the polynomial.

However, in the range of elastic deformations, the transformation function for all types of strain gauges is assumed linear, so equality (3) takes the form:

$$U_c = A\sigma_c + B, \quad (4)$$

where A, B – coefficients that are to be determined according to the results of experimental studies.

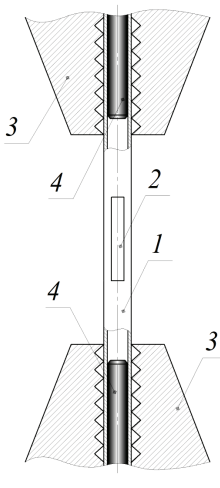

Fig. 5. Scheme of the stand fragment for the calibration of strain gauges: 1 – fragment of the drill string model; 2 – calibration strain gauges; 3 – pincers of a test machine; 4 – steel rod

To establish the explicit form of dependence (4), an experiment is carried out according to the above mentioned method on an P-20 testing machine produced by the USSR (GOST 7855-74), the general view of which is shown in Fig. 6.

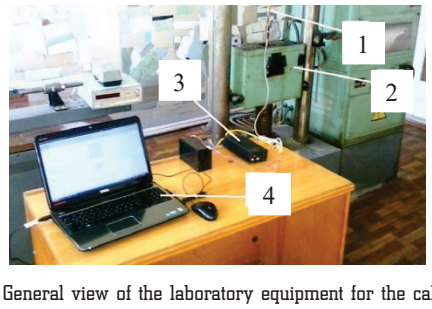

Fig. 6. General view of the laboratory equipment for the calibration of strain gauges: 1 – fragment of the drill string model; 2 – testing machine P-20; 3 – analog-to-digital converter; 4 – personal computer

Analog-to-digital converter, shown in Fig. 2, 6, connected to a personal computer through a USB-interface, using a special driver package.

6. Research results

Therefore, using this stand, laboratory studies of the stress-strain state of a drill string with a diameter of 127 mm are carried out during its operation in the local kink of well No. 10 at the Odesa field (Chornomornaftogaz, Ukraine).

The results of experimental studies for strain gauges that have experienced stretching are presented in Table 1.

Table 1

The results of measuring the stress on the strain gauge model drill string

Position of strain gauges	Voltage, $B \cdot 10^{-2}$				
	Voltage measurement No. 1	Voltage measurement No. 2	Voltage measurement No. 3	Voltage measurement No. 4	Average voltage
1*c*	–0.626	–0.592	–0.558	–0.461	–0.559
2*a*	–0.589	–0.674	–0.576	–0.661	–0.625
3*c*	–0.522	–0.590	–0.613	–0.579	–0.576
1*b*	–0.588	–0.594	–0.544	–0.522	–0.562
2*b*	–0.660	–0.595	–0.548	–0.648	–0.613
3*b*	–0.599	–0.544	–0.764	–0.624	–0.633

An example of a program window for reading data from an analog-to-digital converter in the position of strain gauges «2*a*» (measurement No. 1) is presented in Fig. 7.

To check the results of measurements for uniformity, let's use the *Dickson criterion*, which is used for small samples [12]. To do this, the experimental data must first be placed in the variation series ряд $x_1 \le x_2 \le ... \le x_{n-1} \le x_n$. After that, the extreme left or right values of this variation range are analyzed for *slips*. The formulas for calculating the numerical values of the criteria for checking the extreme values of the variational series for different sample sizes are given in Table 2.

If calculated in the Table 2 values of the criterion is greater than the critical one, then the null hypothesis is rejected and the corresponding extreme value is considered a slip. The critical value of the criterion is found in the table of critical values given in [12].

Therefore, let's determine the values of the calculated Dixon criteria for the extreme values of the variational series, which are formed from the results of 4 measurements for each position of the strain gauges. The results of the calculations are shown in Table 3.

Further, comparing the r_{10} value according to Table 3 with critical values are given in [12] and taken for a sample size of $n=4$ with a confidence level of 0.9; 0.95; 0.99 and 0.995. Statistical analysis shows that measurements that can be qualified as *slips* in this experiment are absent.

The next step, as mentioned above, should be calibrated strain gauges. Photos of samples prepared for the first and second stages of testing are shown in Fig. 8.

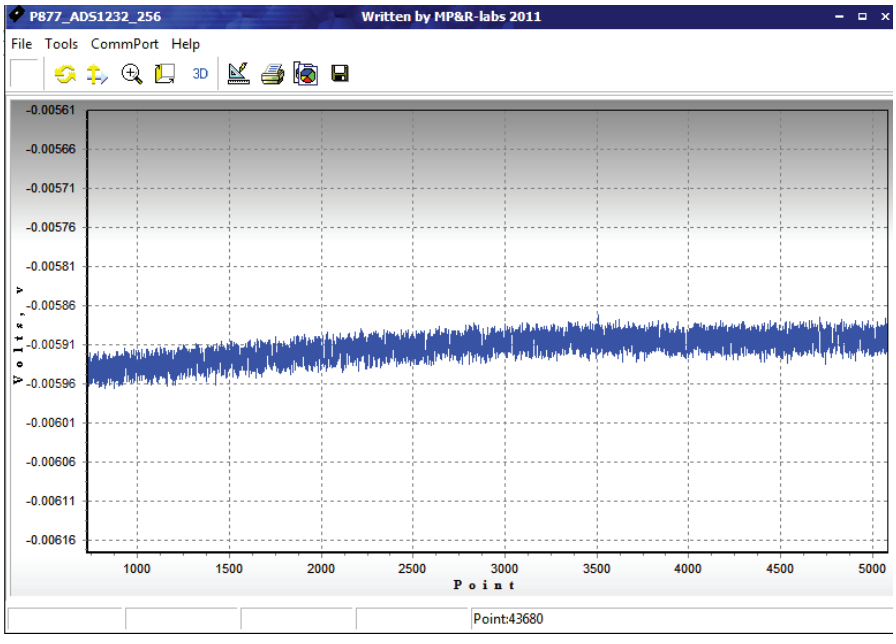

Fig. 7. Screenshot of the program on the results of reading the analog-to-digital converter during the measurement of the No. 1 strain gauge in position «2*a*»

Table 2

Formulas for calculating the numerical values of the criteria for checking the extreme values

Sample size	x_1 slip analysis	x_n slip analysis
$3 \le n \le 7$	$r_{10} = \frac{x_2 - x_1}{x_n - x_1}$	$r_{10} = \frac{x_n - x_{n-1}}{x_n - x_1}$
$8 \le n \le 10$	$r_{11} = \frac{x_2 - x_1}{x_{n-1} - x_1}$	$r_{11} = \frac{x_n - x_{n-1}}{x_n - x_2}$
$11 \le n \le 13$	$r_{21} = \frac{x_3 - x_1}{x_{n-1} - x_1}$	$r_{21} = \frac{x_n - x_{n-2}}{x_n - x_2}$
$14 \le n \le 30$	$r_{22} = \frac{x_3 - x_1}{x_{n-2} - x_1}$	$r_{22} = \frac{x_n - x_{n-2}}{x_n - x_3}$

Table 3

Dixon criteria calculation

Position of strain gauges	Extreme left values, r_{10}	Extreme right values, r_{10}
1*c*	0.588	0.206
2*a*	0.133	0.133
3*c*	0.626	0.253
1*b*	0.306	0.083
2*b*	0.420	0.107
3*b*	0.250	0.636

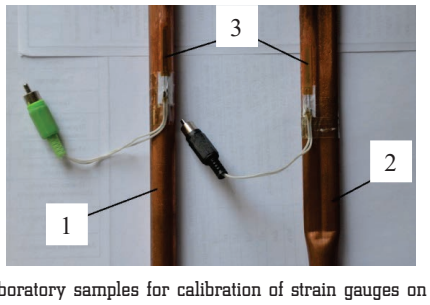

Fig. 8. Laboratory samples for calibration of strain gauges on a tubular model: 1 – calibration sample for the first stage of testing; 2 – calibration sample for the second stage of testing; 3 – strain gauge

Studies were conducted in accordance with GOST 1497-84. Therefore, for each level of tensile strength measurements were performed three times. The results for the first and second stages are presented respectively in Tables 4, 5.

Table 4

The results of the first stage of the calibration of strain gauges

Load, the number of tick marks on the scale	Voltage on calibration strain gauges, V·10^{-2}			
	Voltage measurement No. 1	Voltage measurement No. 2	Voltage measurement No. 3	Average voltage
40	–0.633	–0.637	–0.635	–0.635
50	–0.656	–0.658	–0.658	–0.657
60	–0.685	–0.686	–0.683	–0.685
70	–0.710	–0.709	–0.711	–0.710
80	–0.739	–0.742	–0.743	–0.741
90	–0.766	–0.768	–0.769	–0.768
100	–0.804	–0.800	–0.802	–0.802

Table 5

The results of the second stage of the calibration of strain gauges

Load, the number of tick marks on the scale	Voltage on calibration strain gauges, V·10^{-2}			
	Voltage measurement No. 1	Voltage measurement No. 2	Voltage measurement No. 3	Average voltage
30	–0.587	–0.590	–0.593	–0.590
40	–0.630	–0.631	–0.628	–0.630
50	–0.664	–0.668	–0.666	–0.666
60	–0.688	–0.690	–0.689	–0.689
70	–0.729	–0.727	–0.728	–0.728
80	–0.757	–0.756	–0.758	–0.757
90	–0.786	–0.788	–0.787	–0.787

 ISSN 2226-3780

Using equality from Table 2, the above results of the measurements are analyzed for uniformity according to the Dixon criterion (Tables 6, 7).

Table 6

The values of the calculated Dixon criteria during the first stage of calibration

Load level	Extreme left values, r_{10}	Extreme right values, r_{10}
1	0.5	0.5
2	0.333	0.667
3	0.667	0.333
4	0.5	0.5
5	0.75	0.25
6	0.667	0.333
7	0.5	0.5

Table 7

The values of the calculated Dixon criteria during the second stage of calibration

Load level	Extreme left values, r_{10}	Extreme right values, r_{10}
1	0.5	0.5
2	0.667	0.333
3	0.5	0.5
4	0.5	0.5
5	0.5	0.5
6	0.5	0.5
7	0.5	0.5

Comparison of calculated values of r_{10} with critical values, chosen from [12], testifies to the absence of *slips* among the measurement results.

A screenshot of the program during measurements No. 3 of the first calibration stage, for example, is shown in Fig. 9.

In order to determine the coefficients of the function (4), the data from Tables 4, 5 has been converted to the following form (Tables 8, 9). At the same time, it has been taken into account that laboratory tests are carried out at the price of dividing the tensile testing machine 80 N.

Table 8

Results processing of the first stage of strain gauge calibration

Load, the number of tick marks on the scale	Magnitude of the tensile force, N	Normal stress in cross section, MPa	Average voltage on calibration strain gauges, $V \cdot 10^{-2}$
40	3200	72.76	–0.635
50	4000	90.95	–0.657
60	4800	109.13	–0.685
70	5600	127.32	–0.710
80	6400	145.51	–0.741
90	7200	163.70	–0.768
100	8000	181.89	–0.802

Table 9

Results processing of the second stage of strain gauge calibration

Load, the number of tick marks on the scale	Magnitude of the tensile force, N	Normal stress in cross section, MPa	Average voltage on calibration strain gauges, $V \cdot 10^{-2}$
30	2400	54.57	–0.590
40	3200	72.76	–0.630
50	4000	90.95	–0.666
60	4800	109.13	–0.689
70	5600	127.32	–0.728
80	6400	145.51	–0.757
90	7200	163.70	–0.787

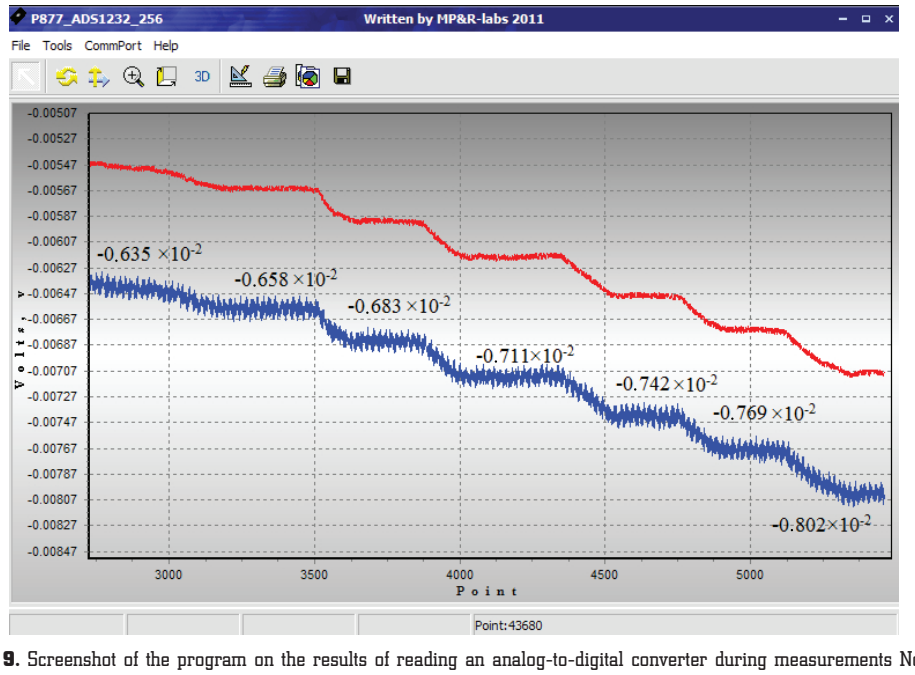

Fig. 9. Screenshot of the program on the results of reading an analog-to-digital converter during measurements No. 3 of the first stage of calibration

As a result, the approximation of the data from the Tables 8, 9, the function (4) acquired the form for the first and second stages of calibration, respectively:

$$U_{c1} = -0.153 \cdot 10^{-4} \sigma_{c1} - 0.519 \cdot 10^{-2}, \quad (5)$$

$$U_{c2} = -0.178 \cdot 10^{-4} \sigma_{c2} - 0.498 \cdot 10^{-2}. \quad (6)$$

Graphically, the data from the Tables 8, 9, and also functions (5) and (6) are shown in Fig. 10.

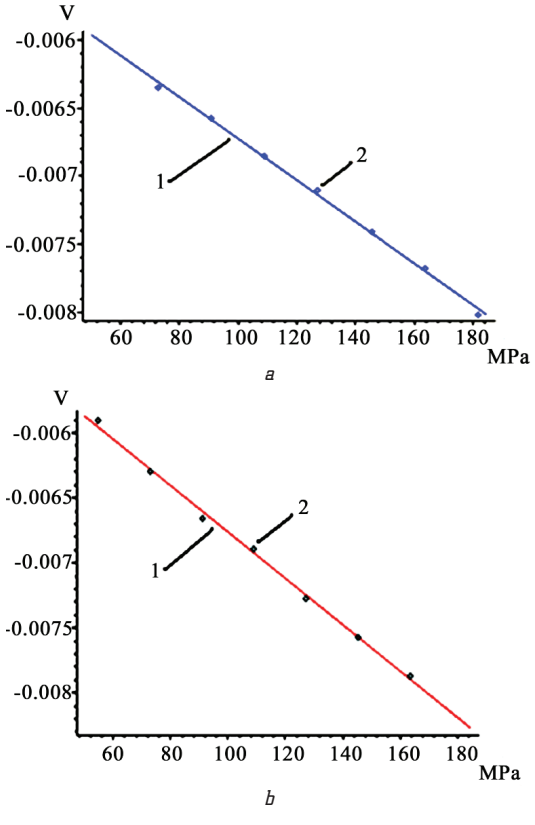

Fig. 10. Graphic interpretation of the dependence of the voltage on the calibration strain gauges from the normal stress in the cross section of the sample: *a* – the results of the first stage of calibration; *b* – the results of the second stage of calibration; 1 – experimental points; 2 – approximating straight line

As expected, the dependencies are of a pronounced straightforward nature.

On the other hand, the difference between the graphs in Fig. 10, *a* and Fig. 10, *b* is not significant. Therefore, we process the results of laboratory studies of the 1st and 2nd stages as one unit. As a result of the approximation, the function (4) will have the following form:

$$U_{c3} = -0.163 \cdot 10^{-4} \sigma_{c2} - 0.511 \cdot 10^{-2}. \quad (7)$$

Let's reflect on one figure all three dependences (5)–(7) together with the experimental points on the basis of which they were obtained (Fig. 11).

As it is possible to see, the maximum deviation of straight lines 2 and 4 from straight line 3 is observed at the very level of stresses (Fig. 11). However, a comparative calculation shows that this deviation does not exceed 3 %. Therefore, on the basis of the above, let's assume that the shape of the surface on which strain gauges are pasted does not affect their readings. Therefore, to describe the relationship between the voltage on the strain gauges and the normal stress in the cross section of the drill string model, let's use function (7).

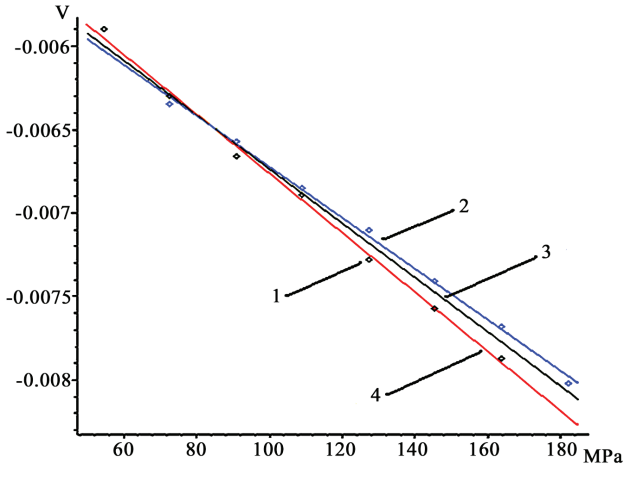

Fig. 11. Graphical interpretation in one graph of the dependence of the voltage on the calibration strain gauges from the normal stress in the cross section of the sample: 1 – experimental points; 2 – approximation dependence on the first stage; 3 – general approximation straight line; 4 – approximation straight line by the second stage

Therefore, taking the average values of the Table 1 and the functional dependence (7), the stresses arising on the surface of the drill string model are calculated. Further, according to the formula:

$$\frac{\sigma_M \mu_M}{q_M} = \frac{\sigma_F \mu_F}{q_F},$$

the magnitudes of the stresses would have occurred in a full-scale drill string. The calculation results are listed in the Table 10.

Table 10

The results of the calculation of the normal stress of bending on the model and the corresponding full-scale drill string

Position of strain gauge	Average voltage, $V \cdot 10^{-2}$	Stress on the surface of the drill string model, MPa	Stress on the surface of the drill string, MPa
1*c*	–0.559	29.6	54.1
2*a*	–0.625	70.2	128.1
3*c*	–0.576	40.1	73.2
1*b*	–0.562	31.5	57.5
2*b*	–0.613	62.8	114.7
3*b*	–0.633	74.9	136.8

Next, let's consider the deformation of the drill string model, obtained in the process of conducting a laboratory experiment. In particular, let's analyze in more detail the mutual position of the copper pipe and the inner surface of the simulator at the three investigated points. To establish the exact placement of the column model, the sizes «*a*» and «*b*» with each of the simulators are measured using a caliper (Fig. 12). Measurement of each size is carried out 4 times according to the method used in reading data

 ISSN 2226-3780

from strain gauges. The results of the experiment are listed in Table 11.

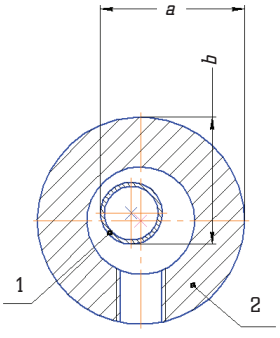

Fig. 12. Measurement of the relative position of the cross sections of the drill string model and the borehole wall simulators: 1 – cross section of the drill string model; 2 – cross section of the borehole wall simulator

Table 11

The results of measuring dimensions «a» and «b» according to Fig. 12

Size	Length, mm				
	Measurement No. 1	Measurement No. 2	Measurement No. 3	Measurement No. 4	Average value
«*a*», sim. No. 1	37.3	35.7	35.9	36.4	36.3
«*b*», sim. No. 1	29.5	29.4	29.8	30.1	29.7
«*a*», sim. No. 2	30.6	30.0	30.3	30.7	30.4
«*b*», sim. No. 2	37.0	37.8	37.9	38.1	37.7
«*a*», sim. No. 3	30.5	29.4	29.1	29.0	29.5
«*b*», sim. No. 3	32.4	31.3	32.7	33.6	32.5

Note: sim. – simulator

By analogy with the measurement results given in Table 1, let's carry out mathematical data processing from Table 11. Consequently, the calculated values of the Dixon criteria are given in Table 12.

Table 12

Dixon criteria calculation

Position of strain gauge	Extreme left values, r_{10}	Extreme right values, r_{10}
1*c*	0.125	0.563
2*a*	0.143	0.429
3*c*	0.429	0.143
1*b*	0.727	0.182
2*b*	0.067	0.733
3*b*	0.478	0.391

All values of the Dixon criteria r_{10} are less than the critical values for a sample of volume $n=4$ with confidence probabilities of 0.95; 0.99 and 0.995 [12]. So among the measured values there are no *slips*.

The mutual position of the drill string model and the borehole wall simulators is shown in Fig. 13. Additionally, for visual comparison, the analytic cross-section positions of the drill string are presented [13].

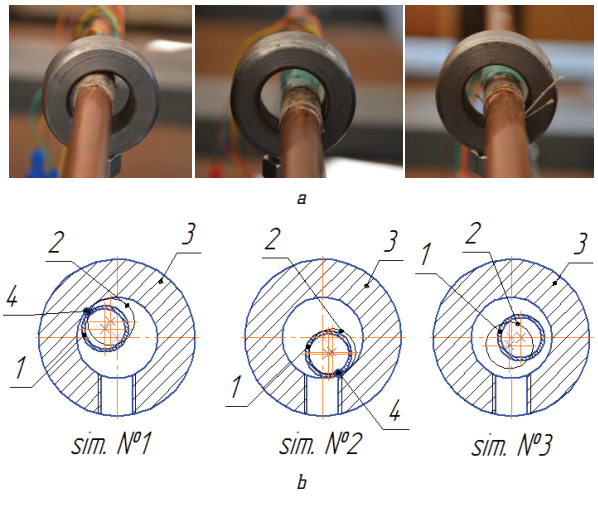

Fig. 13. The mutual position of the cross sections of the drill string model and the borehole wall simulators: *a* – photo; *b* – schematic diagram; 1 – cross section of a drill string model; 2 – contour of the cross-section of the drill string in the position obtained analytically; 3 – cross section of a simulator of a borehole wall; 4 – point of contact between the drill string model and simulators

Let's compare the research results of the stress state of a drill string in the «local bend» of well No. 10 of the Odesa deposit obtained by experimental and theoretical methods.

Let's consider the plane in which the zenith angle changes. As can be seen from the Table 10, the maximum bending stress in the middle of the drill string, obtained using a laboratory experiment, is 128.1 MPa. At the same time, the result of theoretical calculations is 90 MPa [13].

Next, let's analyze the deformation of the drill string in the «local bend» of well No. 10 of the Odesa field, obtained by experimental and theoretical methods (Fig. 13). As it is possible to see, in the qualitative aspect the results of laboratory studies and theoretical calculations coincide. In all three cases, the cross-section of the drill string, obtained by laboratory and experimental methods, are in the same quarters: simulator number 1 – 2nd quarter; simulator number 2 – 4th quarter; simulator number 3 – 4th quarter. Moreover, with the installed placement of simulators, the drill string model contacts only with the 1st and 2nd. A similar result was obtained in theoretical calculations [13]. The reaction on the 3rd simulator is zero, which means that there is no contact on it.

To quantify the deviation between the experimental and theoretical results, let's note that the distance between the centers of sections 1 and 2 (Fig. 13) with their maximum possible deviation from each other can be 11 mm. This value and take for 100 %. The minimum possible distance is 0 mm or 0 %. At the same time, the actual deviations between the cents of these cross sections were 2.9 mm; 1.3 mm and 4.5 mm for each of the simulators, respectively. In general, the difference between experimental and theoretical results is 26 %.

For comparison, let's define the bending stress in the same area of the well, not counting the presence of «local bend». From the results of inclinometric studies, there are:

– length of the curved interval $l_c=180$ m;

– zenith and azimuth angles at the beginning of the interval $\alpha_s=0°$, $\gamma_s=24°$;

– zenith and azimuth angles at the end of the interval $\alpha_e=65°$, $\gamma_e=120°$.

To calculate stresses, let's use the dependencies given in [13]. Therefore, the change in the spatial angle is equal to:

$$\Delta Q = \frac{180^\circ}{\pi}\left(\cos\alpha_s \cos\alpha_e + \sin\alpha_s \sin\alpha_e \sin\left(\gamma_e - \gamma_s\right)\right),$$

$$\Delta Q = 24^\circ.$$

The curvature radius of the well is calculated by the formula:

$$R = \frac{57.3\, l_c}{\Delta Q},$$

$$R = 429.8 \text{ m}.$$

Therefore, the bending stress in the cross section of the drill string:

$$\sigma_b = \frac{Ed}{2R},$$

$$\sigma_b = 0.31 \cdot 10^8 \text{ Pa} = 31 \text{ MPa}. \quad (8)$$

As it is possible to see, the stress in the cross-section of the drill string is determined by the formula (8) without taking into account the «local bend» of the borehole axis up to 4 times less compared to the values obtained in accordance with the experimental method proposed above.

7. SWOT analysis of research results

Strengths. The advantages of the presented experimental method and test bench include the possibility of laboratory modeling of drill pipe strings of any standard sizes. It is also possible to simulate the axes of wells with an arbitrary curvature in a sufficient for practical needs, the range of variation of both zenith and azimuth angles. In addition, the study of models of drill strings instead of full-scale samples will significantly reduce the cost of conducting experiments.

Weaknesses. As a weak side of the developed laboratory equipment, the following can be highlighted:

a) the drill string model can be loaded only with axial tensile force and torque;

b) there is no imitation of tongue and groove joints;

c) the effect of inertial loads on the stress-strain state of the drill string model is not taken into account.

Opportunities. Therefore, further studies should focus on eliminating the above disadvantages, in particular:

– to improve the reference and load nodes of the experimental stand in order to realize also the axial compression load;

– to equip the drill string model with nozzles that are critically similar to the threaded locking joint;

– by dynamic or quasi-dynamic modeling, to take into account when calculating the force and moment of inertia that occur during the rotation of natural drill strings in the well.

Threats. An experimental method has been developed, like any other that requires the cost of the means for their realization. In particular, it is necessary to model each individual size of the drill string with a corresponding copper pipe with a set of strain gauges. In addition, it is necessary to produce simulators of the borehole wall in accordance with the diameter of its trunk for each individual study.

8. Conclusions

1. The proposed experimental stand allows in vitro to investigate the stress-strain state of models of drill pipe strings, taking into account the peculiarities of their location in the local bend of the well. For this, four criteria of similarity between the model of the drill string and its full-scale object are proposed:

1) length of the drill string;

2) axial force acting on the drill string;

3) moment of force in the cross section of the drill string;

4) normal stress in the cross section of the drill string.

2. The design of the stand chassis is designed to simulate an arbitrary value of the intensity of the change in the zenith angle of the well in a local bend. At the same time, the maximum intensity of changes in the azimuth angle is limited exclusively by the width of the chassis and is 24.28°/10 m, which is more than enough for practical needs.

3. In addition, it is possible to load the drill string model with axial tensile force and torque. In addition, the borehole wall simulators limit the transverse movements of the copper pipe, thereby simulating the interaction of the drill string with the bore walls. The effect of the own weight of the drill string is simulated using a special filler in the middle of the copper pipe.

4. Laboratory studies allowed to establish the fact that the normal stress from bending increased 4 times in the cross-section of a 127-mm drill string with its operation in the local bend of well No. 10 of the Odesa field.

In general, it can be argued that the approach proposed in this paper confirms the thesis that the local bend of the borehole axis can significantly increase the bending stress in comparison with the values obtained by generally accepted calculation methods and can be used for practical needs.

References

1. Griguletskiy V. G., Lukyanov V. T. Proektirovanie komponovok nizhney chasti buril'noy kolonny. Moscow, 1990. 302 p.
2. Stiikist i kolyvannia burylnoi kolony / Moisyshyn V. M. et. al. Ivano-Frankivsk, 2013. 590 p.
3. Mitchell R. F. The Effect of Friction on Initial Buckling of Tubing and Flowlines // SPE Drilling & Completion. 2007. Vol. 22, Issue 2. P. 112–118. doi: http://doi.org/10.2118/99099-pa
4. Mitchell R. F. Tubing Buckling–The State of the Art // SPE Drilling & Completion. 2008. Vol. 23, Issue 4. P. 361–370. doi: http://doi.org/10.2118/104267-pa
5. Drillpipe Stress Distribution and Cumulative Fatigue Analysis in Complex Well Drilling: New Approach in Fatigue Optimization / Sikal A. et. al. // SPE Annual Technical Conference and Exhibition. Denver, 2008. doi: http://doi.org/10.2118/116029-ms
6. Helical post-buckling of a rod in a cylinder: with applications to drill-strings / Thompson J. M. T. et. al. // Proceedings of the Royal Society A: Mathematical, Physical and Engineering Sciences. 2012. Vol. 468, Issue 2142. P. 1591–1614. doi: http://doi.org/10.1098/rspa.2011.0558
7. Buckling of a thin elastic rod inside a horizontal cylindrical constraint / Miller J. T. et. al. // Extreme Mechanics Letters. 2015. Vol. 3. P. 36–44. doi: http://doi.org/10.1016/j.eml.2015.03.002
8. Buckling-induced lock-up of a slender rod injected into a horizontal cylinder / Miller J. T. et. al. // International Journal of Solids and Structures. 2015. Vol. 72. P. 153–164. doi: http://doi.org/10.1016/j.ijsolstr.2015.07.025

 ISSN 2226-3780

9. Eksperymentalni doslidzhennia enerhoperedavalnykh funktsii burylnoi kolony u stovburi skerovanoi sverdlovyny / Chudyk I. I. et. al. // Naukovyi visnyk IFNTUNH. 2012. Issue 3 (33). P. 73–80.
10. Stelzer C. Drillpipe Failure and its Prediction: Master Thesis. Leiben, 2007. 115 p.
11. Rachkevych R. V. Laboratorne modeliuvannia deformatsii trubnoi kolony v kryvoliniinomu stovburi sverdlovyny // Naukovyi visnyk IFNTUNH. 2014. Issue 2 (37). P. 68–75.
12. Sverdan P. L. Vyshcha matematyka. Matematychnyi analiz i teoriia ymovirnostei: textbook. Kyiv, 2008. 450 p.
13. Rachkevych R. V. Rozvytok naukovykh osnov zabezpechennia pratsezdatnosti kolon burylnykh i nasosno-kompresornykh trub na diliankakh sverdlovyn iz heometrychnymy nedoskonalostiamy: PhD thesis. Ivano-Frankivsk, 2018. 34 p.

Rachkevych Ruslan, *Doctor of Technical Sciences, Associate Professor, Department of Engineering Mechanics, Ivano-Frankivsk National Technical University of Oil and Gas, Ukraine, e-mail: ruslanvr79@gmail.com, ORCID: http://orcid.org/0000-0003-4113-1907*

Ivasiv Vasyl, *Doctor of Technical Sciences, Professor, Department of Oil and Gas Equipment and Machinery, Ivano-Frankivsk National Technical University of Oil and Gas, Ukraine, e-mail: ivasivvm@i.ua, ORCID: http://orcid.org/0000-0003-4837-1217*

Bui Vasyl, *Head of Laboratories, Department of Engineering and Computer Graphics, Ivano-Frankivsk National Technical University of Oil and Gas, Ukraine, e-mail: vasylbui@gmail.com, ORCID: http://orcid.org/0000-0003-3258-2167*

Yurych Lidiia, *Assistant, Department of Oil and Gas Well Drilling Engineering, Ivano-Frankivsk National Technical University of Oil and Gas, Ukraine, e-mail: lidusiau@ukr.net, ORCID: http://orcid.org/0000-0002-2435-9785*

Rachkevych Iryna, *Postgraduate Student, Department of Oil and Gas Equipment and Machinery, Ivano-Frankivsk National Technical University of Oil and Gas, Ukraine, e-mail: megy@ukr.net, ORCID: http://orcid.org/0000-0002-1313-2200*